New Energy and Future Energy Systems
G.L. Kyriakopoulos (Ed.)

doi:10.3233/AERD220024

The Effect of Leakage Current on the Performance of Proton-Conducting Solid Oxide Fuel Cells

Qiangqiang LI, Yanghui ZHANG, Lili SHEN, Ning ZHAO, Tao ZHANG and Xiaoxia SUN[1]
China North Vehicle Research Institute, Beijing 100072, China

Abstract. In this study, a numerical model is built to analyze the leakage current of a proton conductor solid oxide fuel cell. The transports of electron-hole and proton transfer in a mixed conductor electrolyte is described by the Nernst-Planck equation. The model is validated using experimental data. The leakage current, potential distribution, Faraday efficiency and energy efficiency are analyzed. When the output voltage of the fuel cell is greater than 0.5 V, the leakage current will cause the energy efficiency in a significant reduction. The lower the temperature, the lower the leakage current density. Lowering the temperature will improve the Faraday efficiency and energy efficiency of the fuel cell. Lower output voltage helps improve the Faraday efficiency.

Keywords. Proton conductor solid oxide fuel cell; leakage current; numerical model; Faraday efficiency

1. Introduction

Solid oxide fuel cells (SOFCs) are highly efficient electrochemical energy conversion devices that have the advantages of fuel flexibility, solid state electrolytes, and no need for precious metal catalysts.

Based on the ions conducted by the electrolyte, the SOFCs can be divided into oxygen-conducting SOFCs and proton-conducting SOFCs. Proton conducting solid oxide fuel cells (H-SOFCs) exhibit good protonic conductivity at intermediate temperatures (400-700 °C), because protons are smaller than oxygen ions and they are more likely to pass through the electrolyte, leading to smaller ohmic loss. In addition, because the water steam is generated at the cathode side, the fuel would not be diluted in the anode channels, which makes the H-SOFCs have a high fuel utilization.

H-SOFCs usually use perovskite materials as electrolytes. The electrolytes are usually not pure proton conductors and they are mixed ionic-electronic conductors. The electrolytes typically have two or three mobile charge-carrying defects. By doping with metal cations of low valence, oxygen vacancies are created in the lattice. The oxygen vacancies combine with water steam to generate hydroxide defects through which protons can migrate, making the perovskite materials proton conductive. However,

---

[1] Corresponding author, Xiaoxia Sun, China North Vehicle Research Institute, Beijing 100072, China; E-mail: sun_xiaoxia1983@163.com.

This research was supported by the National Natural Science Foundation of China (Grant No. 52102445).

oxygen vacancies also produce electron-hole ($h^\bullet$) conductivity in an oxidizing atmosphere [1]. Oxygen on the cathode side will greatly increase the electron-hole conductivity. Electron-hole conduction causes the electrons to transfer to cathode via the electrolyte layer, which causes the leakage current. Leakage currents exist even in the open-circuit state, reducing the open-loop potential on the one hand and the current density of the output on the other.

Researchers developed some mathematical models of H-SOFCs with hydrogen [2], methane [3] or ammonia [4] as fuels. In these studies, the effects of cell configuration and operating conditions on the performance of H-SOFCs have been investigated. However, these studies do not take into account current leakage in their models. Based on the chemical equilibrium of defects, Zhu et al. used a Nernst-Planck-Poisson model to develop the theory that can evaluate the open-circuit voltage (OCV) of H-SOFC. The concentration of defects can be estimated using known kinetic parameters. However, these studies mainly focused on the transport of charged defects in the electrolyte, and the effects of defects on the leakage current and performance of whole H-SOFCs have not been extensively investigated.

In this work, we build a 1D model of a H-SOFC to describe the transport of charge and mass in the anode and cathode, and the transport of defects in the electrolyte. The leakage current, potential distribution, Faraday and energy efficiencies of the H-SOFC are analyzed.

2. Mathematical Model

Figure 1 is the diagram of a H-SOFC. The interfaces between the anode, cathode and electrolyte are indicated by Roman numerals I, II, III, and IV. In the anode, hydrogen diffuses to reaction sites occurring the oxidizing reaction:

$$H_2 \rightarrow 2H^+ + 2e^- . \tag{1}$$

Electrons transfer to the cathode via external electrical road. Protons (H^+) from the anode are delivered to the cathode driven by the ionic potential and the defect concentration gradients. At the cathode, oxygen diffuses to reaction sites and reacts with protons to form water with the following reaction equation:

$$O_2 + 4H^+ + 4e^- \rightarrow 2H_2O . \tag{2}$$

Because the electrolyte of the H-SOFC is a mixed conductor of protons and electron holes. Electron holes ($h^\bullet$) can transfer to anode driven by electronic potential.

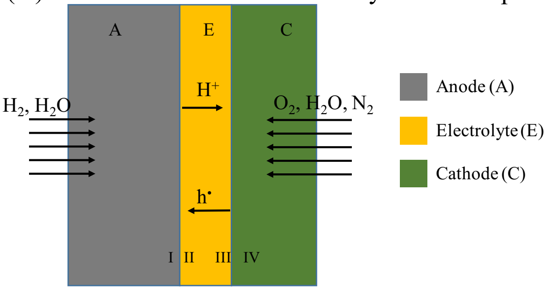

Figure 1. The diagram of a H-SOFC.

In this study, a 1D model is built to describe the charge and mass transfers in the anode and cathode. The Nernst-plank equation is used to describe the transfer of electron holes and proton in the electrolyte layer. Finally, the electrolyte layer is connected with anode and cathode by a boundary coupling at the interfaces I-IV.

2.1. Electrochemical Reaction Dynamics

The electrochemical reaction rates at the anode and cathode can be expressed as a concentration-dependent BV equation:

$$j_{\mathrm{v},i} = j_{0,i} S_{a,i} \left[C_{\mathrm{R}} \exp(\frac{\beta nF}{RT}\eta_{i,\mathrm{act}}) - C_{\mathrm{o}} \exp(\frac{-(1-\beta)nF}{RT}\eta_{i,\mathrm{act}}) \right] \quad i = a, c, \tag{3}$$

where $j_{\mathrm{v},i}$ is the volume reaction current density and $j_{0,i}$ is the exchange current density. $S_{\mathrm{a},i}$ is the active specific surface area. C_{R} and C_{O} are dimensionless expressions, describing the dependence on the reduced and oxidized species in the reaction. $\eta_{i,\mathrm{act}}$ is the active overpotential and is defined as follows:

$$\eta_{i,\mathrm{act}} = \varphi_{\mathrm{el}} - \varphi_{\mathrm{io}} - E_{i,\mathrm{eq}}, \tag{4}$$

$$E_{\mathrm{eq}} = \begin{cases} 0 & \text{Anode} \\ 1.253 - 2.4516\times10^{-4}T + \dfrac{RT}{2F} In(\dfrac{p^0_{\mathrm{H_2}}\sqrt{p^0_{\mathrm{O_2}}}}{p^0_{\mathrm{H_2O}}}) & \text{Cathode} \end{cases}. \tag{5}$$

2.2. Charge Transfer

The transports of e$^-$ and H$^+$ in the anode and cathode can be described by Ohm's Law:

$$\nabla\cdot(\sigma^{\mathrm{eff}}_{\mathrm{el}}\nabla\varphi_{\mathrm{el}}) = \nabla\cdot(-\sigma^{\mathrm{eff}}_{\mathrm{io}}\nabla\varphi_{\mathrm{io}}) = j_{\mathrm{v}} \tag{6}$$

where $\sigma^{\mathrm{eff}}_{\mathrm{io}}$ and $\sigma^{\mathrm{eff}}_{\mathrm{el}}$ are the effective ionic and electronic conductivity, respectively.

In the electrolyte layer, protons are conducted from the anode to the cathode driven by the ionic potential gradient and their own concentration gradient. Electron holes are conducted from the cathode to the anode by the electron potential gradient and their own concentration gradient, and are neutralized with electrons at the anode-electrolyte layer interface. This behavior of electron holes causes a decrease of electrons produced at the anode and the formation of a leakage current. The fluxes (j_i, unit: mol/(m^2·s)) of these charges are described by the Nernst-Planck equation:

$$j_{\mathrm{H^+}} = -D_{\mathrm{H^+}}\nabla c_{\mathrm{H^+}} - \frac{\sigma_{\mathrm{H^+}}}{z_{\mathrm{H^+}}F}\nabla\varphi_{\mathrm{io}} \tag{7}$$

$$j_{\mathrm{h^\bullet}} = -D_{\mathrm{h^\bullet}}\nabla c_{\mathrm{h^\bullet}} - \frac{\sigma_{\mathrm{h^\bullet}}}{z_{\mathrm{h^\bullet}}F}\nabla\varphi_{\mathrm{el}} \tag{8}$$

where the first term represents the charge migration due to charge density gradient. It should be noted that the unit of charge density c_i is mol/m^3. And second term represents charge migration due the ionic potential gradient, i.e. Ohm's law. D_i (unit: m^2·s) is the diffusion coefficient:

$$D_i = \frac{RT}{(z_i F)^2 c_i}\sigma_i\,. \tag{9}$$

Substituting Eqs. (9) into Eqs. (7) and (8), we have:

$$j_i = -\frac{1}{(z_iF)^2}\sigma_i \nabla RT\ln c_i - \frac{\sigma_i}{z_iF}\nabla\varphi_i \tag{10}$$

The chemical potential, μ, (unit: J/mol), is related to the concentration of the specific species as:

$$\mu_i = \mu_i^0 + RT\ln c_i \tag{11}$$

Substituting Eqs. (11) into Eq. (10), and using the equation $J_i = z_iFj_i$, the current densities J_i (unit: A·m^{-2}) is obtained as:

$$J_i = -\frac{\sigma_i}{z_iF}\nabla\mu_i - \sigma_i\nabla\varphi_i \tag{12}$$

According to the definition of electrochemical potential, we have:

$$\overline{\mu_i} = \mu_i + z_iF\varphi_i \tag{13}$$

$$J_i = -\frac{\sigma_i}{z_iF}\nabla\overline{\mu_i} \tag{14}$$

According to the electrochemical balance, we have:

$$\overline{\mu}_{H^+} = 0.5\mu_{H_2} - \overline{\mu}_{e^-} \tag{15}$$

$$\overline{\mu}_{h^\cdot} = -\overline{\mu}_{e^-} \tag{16}$$

Then the ionic current density is:

$$J_{io} = -\frac{\sigma_{H^+}}{2F}\nabla\mu_{H_2} - \sigma_{H^+}\nabla\psi_{io} \tag{17}$$

The leakage current density is:

$$J_{leakage} = J_{h^\bullet} = -\sigma_{h^\bullet}\nabla\psi_{el} \tag{18}$$

where $\psi_i = (\mu_i - F\varphi_i)/(-F)$ [5]. Assuming no homogenous reactions in the electrolyte, the governing equations for the two species become:

$$\nabla\cdot J_{io} = \nabla\cdot J_{h^\bullet} = 0. \tag{19}$$

Faraday efficiency η_{Fa} and energy efficiency ω are defined as:

$$\eta_{Fa} = \frac{J_{io} - J_{leakage}}{J_{io}}, \tag{20}$$

$$\omega = \frac{2FV_{cell}}{LHV}\eta_{Fa}, \tag{21}$$

where LHV is the low heating value of hydrogen.

2.3. Mass Transfer

The pressure gradient has little effect on mass transfer. Mass transfer is mainly caused by the substance concentration gradient. [6]. The total pressures of the anode and cathode are assumed to be constant in this study. Wilke-Bosanquet model is used to describe the diffusion in electrodes[7]:

$$\nabla \cdot (-D_i^{\mathrm{eff}} \nabla C_i) = s_i , \tag{22}$$

The diffusion coefficient D_i^{eff} is calculated from the ordinary diffusivity $D_{\mathrm{mix},i}$ and the Knudsen diffusivity $D_{\mathrm{Kn},i}$ [7]:

$$D_i = \frac{\xi}{\tau_{\mathrm{pore}}} \left(\frac{1}{D_{\mathrm{mix},i}} + \frac{1}{D_{\mathrm{Kn},i}} \right)^{-1} . \tag{23}$$

s_i^{tpb} denotes the mass source per volume and is expressed as:

$$s_{\mathrm{H_2}} = -\frac{j_{\mathrm{v,a}}}{2F} , \tag{24}$$

$$s_{\mathrm{H_2O}} = \frac{j_{\mathrm{v,c}}}{2F} , \tag{25}$$

$$s_{\mathrm{O_2}} = \frac{j_{\mathrm{v,c}}}{4F} . \tag{26}$$

2.4. Boundary Conditions

Table 1 gives the boundary conditions in this study. Anode is feed with H_2 containing 3% H_2O. H_2O does not participate the electrochemical reaction of anode. Cathode is fed with wet air containing 3% H_2O. The temperature of the button cell is assumed to be uniform, thus ignoring the energy equation.

Table 1. Boundary conditions.

Positions	Total pressure (atm)	Mass transfer	Charge transfer
A-E interface	1	97% H_2+3% H_2O	$\varphi_{\mathrm{el}} = 0$
C-E interface	1	20% O_2+3% H_2O+77% N_2	$\varphi_{\mathrm{el}} = V_{\mathrm{cell}}$

Because leakage current flow through the electrolyte layer, there is electrical potential in the electrolyte layer. In the anode-electrolyte and cathode-interface of Figure 1, we have continued changes of the ionic potential and chemical potential: $\varphi_{\mathrm{ion}}^{\mathrm{I}} = \varphi_{\mathrm{ion}}^{\mathrm{II}}$, $\varphi_{\mathrm{ion}}^{\mathrm{III}} = \varphi_{\mathrm{ion}}^{\mathrm{IV}}$, $\varphi_{\mathrm{el}}^{\mathrm{I}} = \varphi_{\mathrm{el}}^{\mathrm{II}}$, $\varphi_{\mathrm{el}}^{\mathrm{III}} = \varphi_{\mathrm{el}}^{\mathrm{IV}}$, $\mu_{\mathrm{H_2}}^{\mathrm{I}} = \mu_{\mathrm{H_2}}^{\mathrm{II}}$, $\mu_{\mathrm{H_2}}^{\mathrm{III}} = \mu_{\mathrm{H_2}}^{\mathrm{IV}}$.

3. Results and Discussion

Liu et al.[8] experimentally tested the performance of a button H-SOFC with a configuration of BZCY17-Ni/BZCY17/LSCF. Anode was fed with 3% H_2O/97% H_2, while the cathode was fed with wet air containing 3% H_2O. The parameters of the H-SOFC are listed in Table 2.

Table 2 Parameters of the H-SOFC [8].

Parameters	Anode	Cathode	Electrolyte
Thickness (μm)	550	40	15
Porosity	0.3	0.3	–
Pore diameter(μm)	1	1	–
Tortuosity	3	3	–

Figure 2(a) shows the comparison of numerical results with experimental results. It can be found that our modeling results agree well with the experimental data. As the operating temperature increases, the open-circle voltage (OCV) of the H-SOFC decreases. Table 3 lists the simulated OCVs. It can be found that simulated OCVs are lower than theoretical OCVs because of the leakage current. Figure 2(b) shows the effect of molar fraction of oxygen on the fuel cell performance. It can be found that increasing molar fraction of oxygen helps to increase the OCV and the current density of H-SOFC. The increase of current density is mainly cause by the increase of OCV. The effect of concentration polarization is weak because the cathode is too thin and thus O_2 is enough.

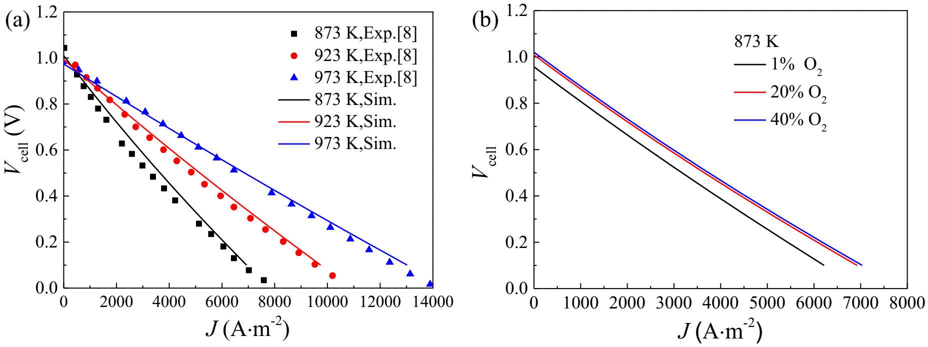

Figure 2. Effects of the temperature and the molar fraction of oxygen on the performance of H-SOFC: (a) the effects of the temperature; (b) the effects of the molar fraction of oxygen.

Table 3 OCVs at different temperatures.

Temperature (K)	**873**	**923**	**973**
Theoretical OCV (V)	1.14	1.134	1.127
Simulated OCV (V)	1.01	0.99	0.97

Figure 3 shows the electronic potential and ionic potential distribution in the H-SOFC with the output voltage of 0.7 V. the figure only shows the distributions at the vicinity of electrolyte layer. It can be found the due to the existence of the leakage current, there is electronic potential in the electrolyte layer. This potential gradient drives the transport of the electrons. The electron potentials at different temperatures are almost equal. And there is a slight difference in the ionic potential at different temperatures, implying that temperature has a significant effect of ionic current and affects the transport of H^+.

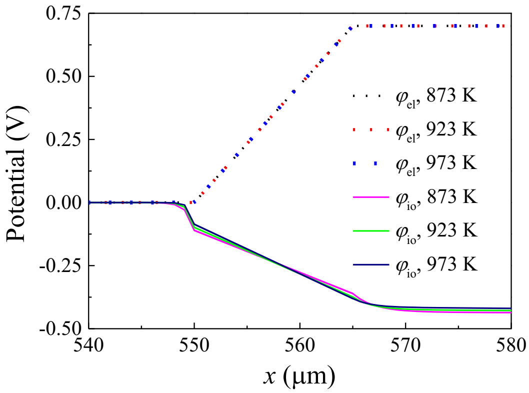

Figure 3. The electronic potential and ionic potential distribution in the H-SOFC.

Figure 4 shows the effect of temperature on the leakage current density and Faraday efficiency. It can be seen that the leakage current density is of the same magnitude as the output current density and is not negligible. The leakage current increases with the increase of output voltage. And the higher the temperature, the faster the growth rate, which is due to the fact that increasing the temperature causes the conductivity of electron holes to increase. The presence of leakage current leads to a decrease in the Faraday efficiency of the fuel cell. It can be seen that the Faraday efficiency of the fuel cell decreases as the output voltage and the operating temperature increase. In particular, the Faraday efficiency decreases sharply when the voltage approaches OCV.

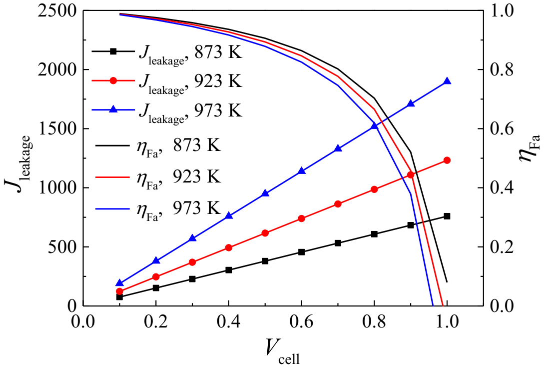

Figure 4. Effect of temperature on the leakage current density and Faraday efficiency.

Figure 5 shows the theoretical (ηFa = 100%) and the actual energy efficiencies of the H-SOFC at different output voltages. When the current leakage is zero, Faraday efficiency is 100%. Under this condition, the energy efficiency ω of the cell is proportional to the output voltage. The higher the output voltage, the greater the energy efficiency. When the output voltage is very high and the current density is very small, the consumed hydrogen is mainly converted into electric power, so the energy efficiency is high. However, the H-SOFC generates leakage current in actual operation. The leakage current makes the actual energy efficiency less than the theoretical energy efficiency, especially at high output voltages (>0.8 V), because the leakage current does not go through the external circuit but directly to the cathode. At low output voltages (<0.4V), the energy efficiency of the fuel cell is almost the same as the theoretical value because the leakage current density is very small. In addition, the energy efficiency decreases with increasing operating temperature.

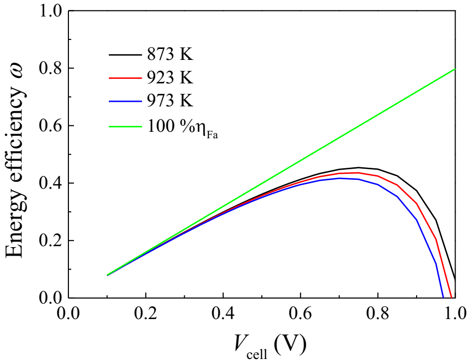

Figure 5. The effect of temperature on the energy efficiency of H-SOFC.

4. Conclusion

In this study, a numerical model is built to analyze the leakage current of a proton conductor solid oxide fuel cell. The transports of electron-hole and proton transfer in a mixed conductor electrolyte is described by the Nernst-Planck equation. The model is validated using experimental data. The leakage current, potential distribution, Faraday efficiency and energy efficiency of the cell are analyzed. When the output voltage of the fuel cell is greater than 0.5 V, the leakage current will cause the energy efficiency in a significant reduction. The lower the temperature, the lower the leakage current density. Lowering the temperature will improve the Faraday efficiency and energy efficiency of the fuel cell. Lower output voltage helps improve the Faraday efficiency.

References

[1] Lefebvre-Joud F, Gauthier G, and Mougin J. Current status of proton-conducting solid oxide fuel cells development. Journal of Applied Electrochemistry, 2009; 39(4):535-543.

[2] Zhang JH, Lei LB, Liu D, Zhao FY, Ni M, and Chen F. Mathematical modeling of a proton-conducting solid oxide fuel cell with current leakage. Journal of Power Sources, 2018; 400:333-340.

[3] Menon V, Banerjee A, Dailly J, and Deutschmann O. Numerical analysis of mass and heat transport in proton-conducting SOFCs with direct internal reforming. Applied energy, 2015; 149:161-175.

[4] Kalinci Y and Dincer I. Analysis and performance assessment of NH3 and H2 fed SOFC with proton-conducting electrolyte. International Journal of Hydrogen Energy, 2018; 43(11):5795-5807.

[5] Shen S, Guo L, and Liu H. An analytical model for solid oxide fuel cells with bi-layer electrolyte. International Journal of Hydrogen Energy, 2013; 38(4):1967-1975.

[6] Williford RE, Chick LA, Maupin GD, Simner SP, and Stevenson JW. Diffusion limitations in the porous anodes of SOFCs. Journal of the Electrochemical Society, 2003; 150(8): A1067-A1072.

[7] Andersson M, Yuan JL, and Sunden B, SOFC modeling considering electrochemical reactions at the active three phase boundaries. International Journal of Heat and Mass Transfer, 2012; 55(4):773-788.

[8] Qiu R, Lian W, Ou Y, Tao Z, Cui Y, Tian Z, Wang C, Chen Y, Liu J, and Lei L. Multifactor theoretical analysis of current leakage in proton-conducting solid oxide fuel cells. Journal of Power Sources, 2021; 505:230038.